

Supporting Information

Nanocubes Composed of FeS_2 @C Nanoparticles as a High-Capacity Anode Material for K-ion Storage

Yushan Luo, Mengli Tao Jianhua Deng, Renming Zhan, Bingshu Guo, Qianru Ma, Muhammad Kashif Aslam, Yuruo Qi* and Maowen Xu*

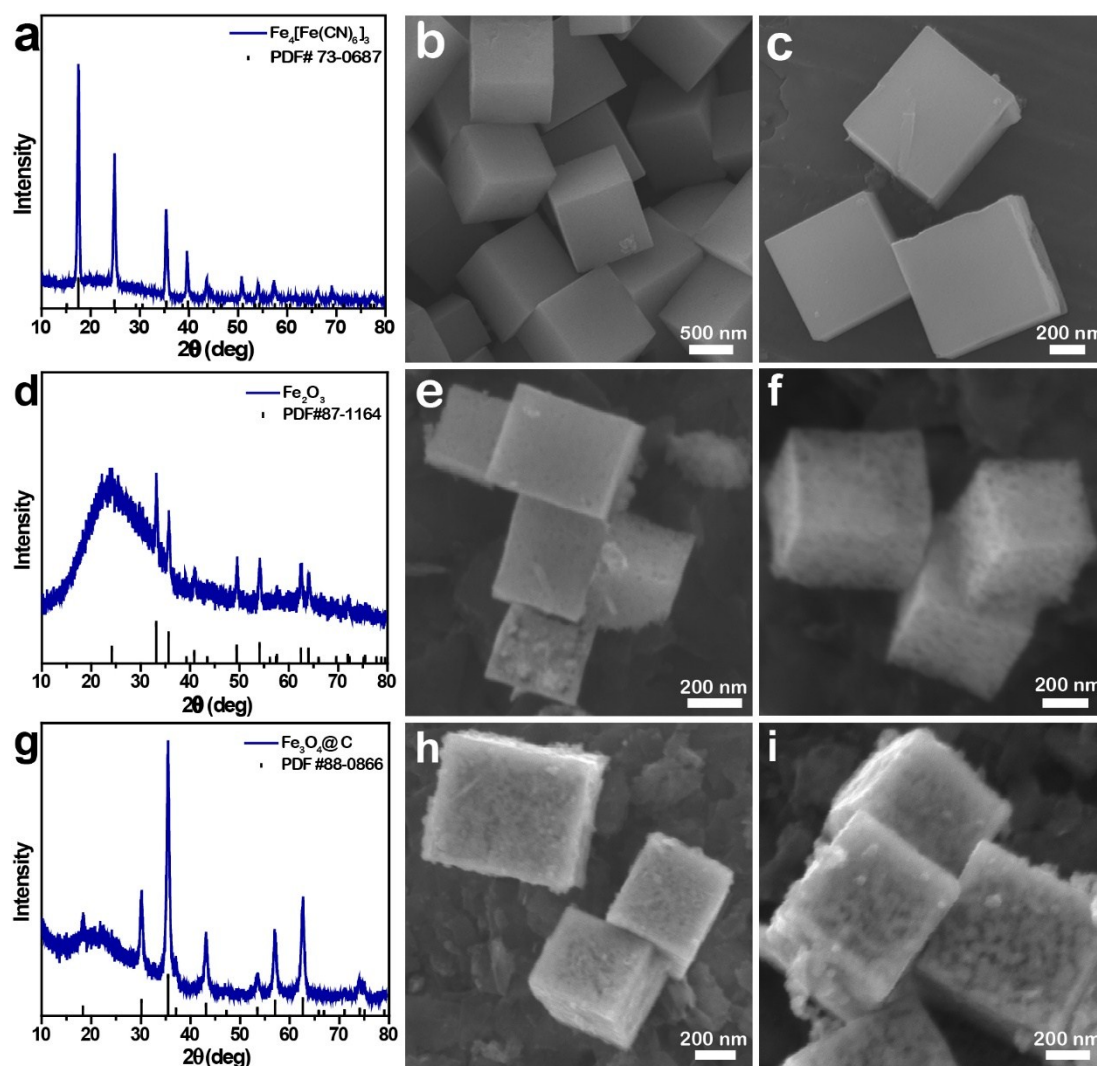


Figure S1. XRD patterns and morphologies of precursors: a) PB corresponding XRD and b, c) SEM images of PB; d) Fe_2O_3 corresponding XRD and e, f) SEM images of Fe_2O_3 ; g) Fe_3O_4 @C corresponding XRD and f-i) SEM images of Fe_3O_4 @C through etching process.

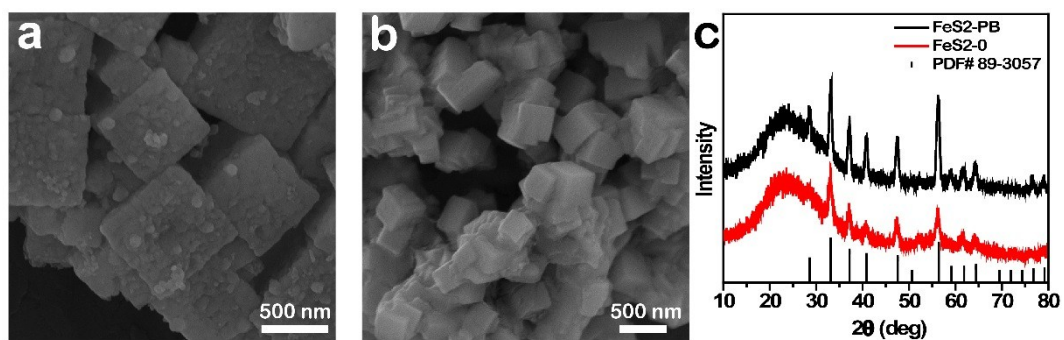


Figure S2. Morphology and structure of comparative samples. SEM images of a) $\text{FeS}_2\text{-0}$, b) $\text{FeS}_2\text{-PB}$ and c) corresponding XRD patterns.

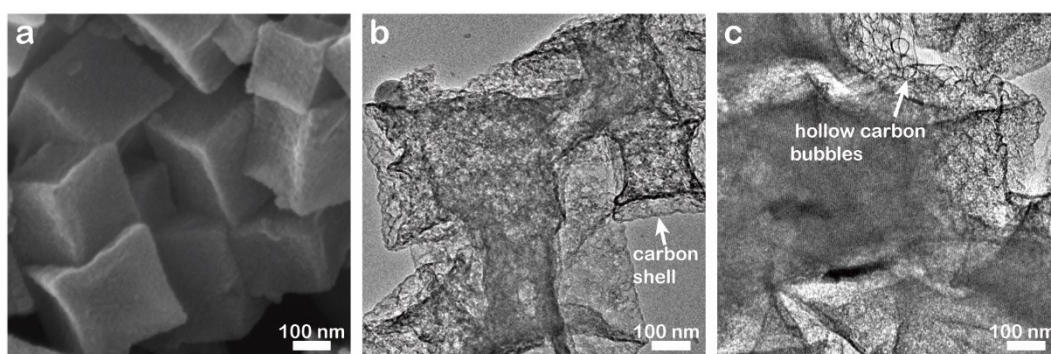


Figure S3. FESEM and TEM images of $\text{FeS}_2\text{@C}$ composite: carbon shell and hollow carbon bubbles have been left after etching with 4M HCl for 30min.

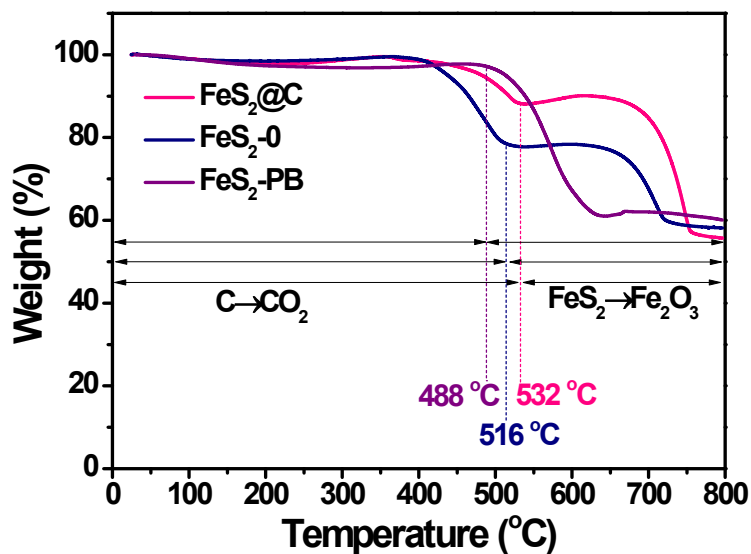


Figure S4. TGA curves of FeS₂@C, FeS₂-0 and FeS₂-PB.

TGA analysis were carried out to evaluate the carbon content in the composite, as shown in Figure S4. There are two stages in the TGA curves. Carbon is lost during the first stage, while the second stage is mainly derived from the transition of FeS₂ to Fe₂O₃. According to the first stage of TGA curves, the carbon content of FeS₂-PB, FeS₂@C and FeS₂-0 is calculated to be around 2.7%, 11.6% and 21.5%. Because the FeS₂-PB sample was obtained from the direct sulfuration of the PB precursor without any carbon coating, the carbon content of FeS₂-PB is negligible. Therefore the FeS₂-PB exhibits a different weight-loss behavior because the first stage of FeS₂-PB is not obvious.

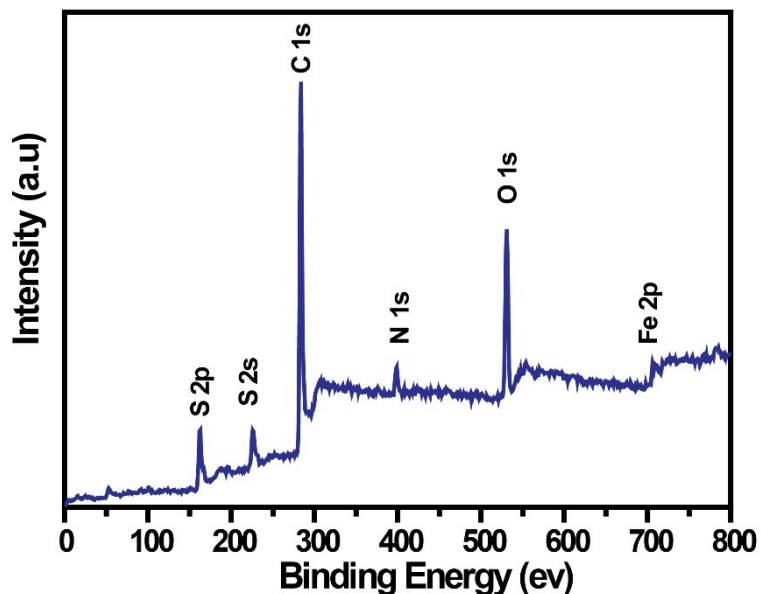


Figure S5. XPS survey spectrum of the FeS₂@C nanocubes.

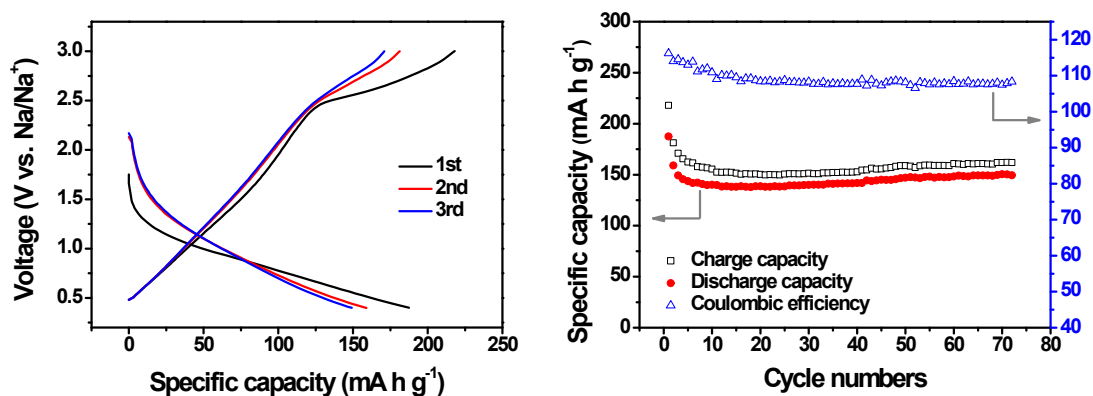


Figure S6. Discharge/charge curves and cycling performance of the carbon shell derived from PDA at 0.5 A g⁻¹.

The specific capacity of the carbon derived from PDA was evaluated by K half cells. As displayed in Figure S6, the discharge capacity in the second cycle (because decomposition of electrolyte was observed in the first charge curves at above 2.45 V) is about 158 mA h g⁻¹. Taking the carbon content (11.6%) of FeS₂@C into consideration, the capacity contribution of the carbon shell is 18.3 mA h g⁻¹.

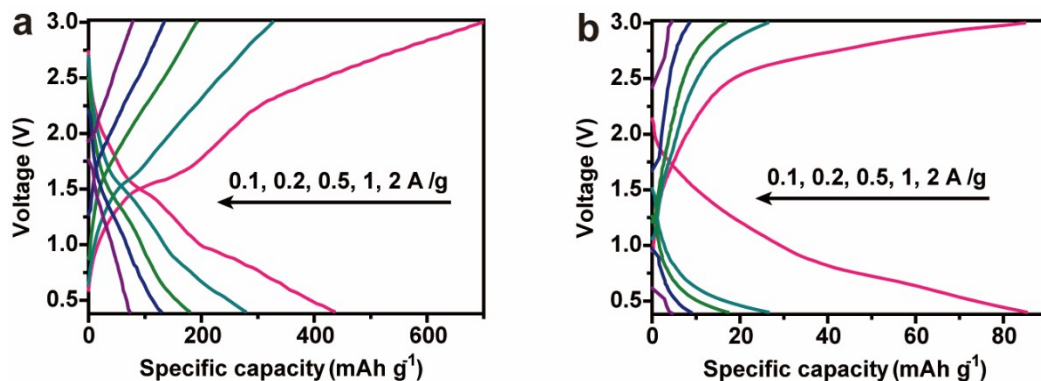


Figure S7. Discharge/charge profiles at various current densities from 0.1 mA g⁻¹ to 2 A g⁻¹: a) FeS₂-0; b) FeS₂-PB.

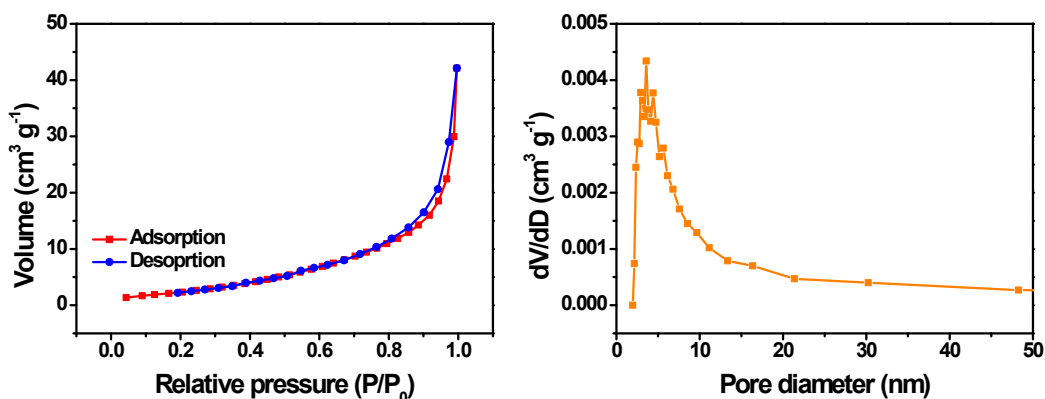


Figure S8. Nitrogen adsorption/desorption isotherms and corresponding pore diameter distribution of the as-synthesized FeS₂@C nanocube.

The nitrogen adsorption/desorption isotherms and pore distribution of the as-synthesized sample were shown in Figure S8. The Brunauer-Emett-Teller (BET) specific surface area is about 10.3 m² g⁻¹ and the average pore size is around 5 nm. The limited specific surface area is not sufficient to supply large amount of surface active sites. However, this kind of core-shell nanocubes with mesoporous constructed by numbers of nanoparticles may be beneficial for the penetration of electrolyte and

diffusion of Na⁺ ions. Thus, the K storage behavior of the as-synthesized sample is contributed by both capacitive and diffusion process, which is coincide with the calculated capacitive contribution ratio (Figure 5c-d).